We faced similar problem while observing the sun-dial at Hyder Ali's tomb. One of the minarets erected later in the neighbourhood blocks incidence of sun light on the dial for a significant duration of the day. This problem is obvious in Figure 1 *a* also.

1. Balasubramaniam, R. and Dass, M. I., On the astronomical significance of the Delhi Iron Pillar. *Curr. Sci.,* 2004, **86**(5), 1134–1142.
2. Pandya, A., Bahadur, T. and Bhattacharya, S., Time keeping in the past: sun-dial in Jaisalmer Fort. *Indian J. Hist. Sci.*, 2017, **52**(2), 138–147.
3. Gatty, A., *The Book of Sun-Dials*, George Bell and Sons, London, 1872, pp. 1–2; http://digital.library.upenn.edu/women/gatty/sundials/sundials.html
4. Kaye, G. R., The astronomical observatories of Jai Singh, *Arch. Surv. India*, New Imperial Series, 1973, **XL**.
5. Singh, P., *Indian and Islamic Stone Observatories*, Holiday Publications, Jaipur, 2009
6. Singh, P., *Stone Observatories of India*, Bharat Manisha, Varanasi, 1975.
7. Kochar, R. and Narlikar, J., *Astronomy in India*, Indian National Science Academy, New Delhi, 1994, pp. 6–9.
8. Kochar, R. and Narlikar, J., Astronomy in India: Past, present and future, Inter University Centre for Astronomy and Astrophysics, Pune, and Indian Institute of Astrophysics, Bangalore, 1993, pp. 11–18.
9. Heritage of the Mysore division, The District Gazetteers of Mysore and Mandya, Deptt. of Gazetteer, Bangalore, http://rcmysore.gov.in/heritage.pdf
10. Sheik Ali, B., *Tipu Sultan: A Crusader for Change*, Knowledge Publication Society, Mysuru, 2014, pp. 390–391; www.bshekali.in
11. Abdul Karim, S. M., *A Guide to PRAYER in Islam*, The Co-operative Office for Call and Foreigners' Guidance at Sultanah, Riyadh, 1997, pp. 16–17; http://www.islamicbook.ws/english/english-020.pdf
12. For computer programme to calculate prayer time of *Asr*: http://astronomyaardra.org/res.htm

ACKNOWLEDGEMENTS. We thank the Archeological Survey of India (ASI), Bangalore Circle, and the authorities of Jamia Masjid and Gumbaz at Srirangapatna for permission. We also thank Prof. B. Sheik Ali and Prof. Karimuddin for explaining the rationale of a sun-dial in a mosque and the history of Jamia-Masjid and the Hyder Ali's tomb in Srirangapatna.

Received 4 April 2017; revised accepted 16 January 2019

doi: 10.18520/cs/v116/i5/811-816

Impact of Cartosat-1 orography in 330 m Unified Model forecast

A. Jayakumar*, Jisesh Sethunadh, Timmy Francis, Saji Mohandas and E. N. Rajagopal

National Centre for Medium Range Weather Forecasting, Ministry of Earth Sciences, Government of India, A-50, Sector 62, Noida 201 309, India

The newly introduced high-resolution (330 m) regional model, Delhi Model (DM), at the National Centre for Medium Range Weather Forecasting targets winter time fog/visibility forecast over Delhi, India. The present study focuses on the benefits of enhanced orographic features in DM, through a new data set developed using the Indian Space Research Organisation Cartosat-1 orography (Cartosat-run), against those from the NASA Shuttle Radar Topography Mission Digital Elevation Model employed previously (SRTM-run). The early morning visibilities from the Cartosat-runs were lower compared to the SRTM-runs, which could be linked to an enhanced downdraft (negative vertical velocity) in the former, helping form a shallow and stratified boundary layer. The evolution and variability of 'ventilation index' in the model domain is regulated by the local wind circulation changes within the shallow boundary layer which in turn is modulated by the orography representation. The DM forecasted ventilation index has been projected to be a potential indicator of the atmosphere dispersion of airborne pollutants over Delhi.

Keywords: Cartosat, fog, orography, visibility.

SOCIO-ECONOMIC vulnerability to the poor visibility conditions in Delhi under extended and heavy fog spells during winter period exacerbates with the exorbitant conditions of poor air quality. Observational study by Ghude *et al.*[1] shows that the increasing trend in fog days/hours over Indian cities is linked with enhanced urban aerosol loading and moisture availability. Conversely, the urban heat island (UHI) effect manifests itself as a gradient in the aforementioned fog trends between urban and suburb regions[2]. The Government of India has initiated intensive ground-based measurement campaigns such as WIFEX[1], with a view to developing improved fog/visibility forecast capabilities in varying spatio-temporal scales. Better representation of land–atmosphere coupling and various physical processes is crucial to improving the fog/visibility forecast skills[3].

Here we have focused on improving visibility forecasting in the National Centre for Medium Range Weather Forecasting's (NCMRWFs) high-resolution Unified Model

*For correspondence. (e-mail: jkumar@ncmrwf.gov.in)

set-up at 330 m grid length over a small domain around Delhi (hereafter DM)[4] by representing the surface boundary conditions at fine resolution. DM is able to reproduce the spatial variability in observed visibility and the UHI characteristics are more realistic than the coarse resolution models. On the other hand, the minimum visibility values for the season predicted by the model are statistically higher compared to the observations[4]. Since fog is highly conditioned by the finer resolution of the terrain and local landscape features, the present work focuses on the impact of orography data, generated from the Indian Space Research Organisation (ISRO) Cartosat-1 digital elevation model (DEM) with a source resolution of ~30 m, on the fog/visibility forecast using DM.

The Cartosat-1 satellite, launched in May 2005, provides high-quality data for topographic applications. Cartosat-1 DEM high-resolution data have been digitally generated from Cartosat-1 observations and are available from the Bhuvan geoportal of ISRO. These data produce more accurate values of elevation for peaks and valleys, which are highly important for the horizontal accuracy in fog prediction. Patel *et al.*[5] found that the Cartosat-1 DEM has higher quality and outperformed other sources of DEM for topographical consistency in the Indian domain. Sethunadh *et al.*[6] studied the impact of Cartosat-1 DEM in NCMRWF high-resolution model using 1.5 km grid resolution over Chennai region. The results were encouraging in providing a realistic representation of heavy precipitation through localized wind convergence and persisting cloud cover over that location.

DM is a triple-nested model, and results from the innermost nested domain with a grid length of 330 m have been used here for detailed analysis. DM covers a domain of 100 km × 100 km and uses 80 vertical levels with model top at 38.5 km and 14 model levels below 1 km. The model configuration and science details, including visibility parameterization are discussed in Jayakumar *et al.*[4]. In the present study, the mean orography for the inner domain is generated from two different sets of data, NASA SRTM DEM (hereafter SRTM) and ISRO Cartosat DEM (hereafter Cartosat), whereas the driver model orography is maintained free from any modifications. Figure 1 *a* and *b* shows the orography generated from Cartosat and SRTM respectively, while Figure 1 *c* gives the difference between the two. Topography of this domain mainly includes Yamuna flood plains and the Delhi ridge, which is a northern extension of the Aravallis with a peak elevation of 320 m. Significant differences are found over the eastern sector of the domain. Maximum elevation is over the southern ridge of the Aravalli range. Detailed discussions on the implementation of the Cartosat orography in the NCMRWF high-resolution Unified Model can be found in Sethunadh *et al.*[6] The geoid undulation corrected data are bilinearly interpolated to the model grid and use a 1-2-1 filter to avoid numerical instability, following the work by Sethunadh *et al.*[6] The present study employs model runs performed using both SRTM DEM (hereafter SRTM-run) and Cartosat DEM (hereafter Cartosat-run) orography for the fog cases, based on 00 UTC initial conditions of 8 January and 2 February 2017, with a forecast lead time of 36 h.

Figure 1 *d* shows forecast from both these runs for visibility, temperature and relative humidity (RH) along with the Metar observation data of the Indira Gandhi International Airport (IGIA), New Delhi. The drop in visibility – similar to that in the observation – is seen from 12 UTC, and this temporal pattern is captured reasonably well in the model. However, noticeable difference of more than 2°C in temperature between model and observation is reflected in the visibility forecast. There is no significant difference for the aforementioned parameters between Cartosat and SRTM runs over the IGIA due to the fact that the difference in elevation between the two datasets is negligible over IGIA (Figure 1 *c*). Despite the fact that the IGIA differences are small, the difference in these variables depicted in the spatial plots for 2 UTC on 9 January and 3 February 2017, is a clear evidence of the impact of Cartosat over DM (Figure 2). A visibility difference with a maximum value of 200 m during morning hours is generally consistent over the region characterized by a positive elevation in Figure 1 *c*. While in the present study, fog is defined under the classification of visibility values less than 1000 m, a difference of 200 m in visibility value could be considered statistically significant. Low temperature along with availability of moisture supply support fog growth. This is evident in the spatial 'difference' plots between the two cases; a subtle distinction in temperature and RH values, which qualitatively shows the prominent impact of Cartosat implementation in DM. Spatial verification of RH from both the runs against the automatic weather station (AWS) observation can be found in the Supplementary Figure 1. There are regions in the model where RH values are consistent with the AWS observation, though unfortunately, there are no AWS observations available over regions where significant orographic variations exist between Cartosat-run and SRTM-run in the model domain.

Figure 3 illustrates histograms of temperature, RH and visibility, which provide quantitative information on the distribution of these variables on the DM grids during morning hours. The entire DM domain is considered here for the histogram calculations. Since fog is defined below 1000 m visibility, Figure 3 *a* is selected only for the bins less than this threshold value. Except 0.8 m with an insignificant measure of probability density function, other bins point out the characteristics of fog with considerable amount of significance in the frequency of occurrence. Consistent with the visibility information, histograms of surface temperature and RH give maximum distributions above a threshold limit of 12.35°C and 90% respectively, of the selected case periods. In contrast to Cartosat-run distribution, SRTM-run is tailored towards the distribution

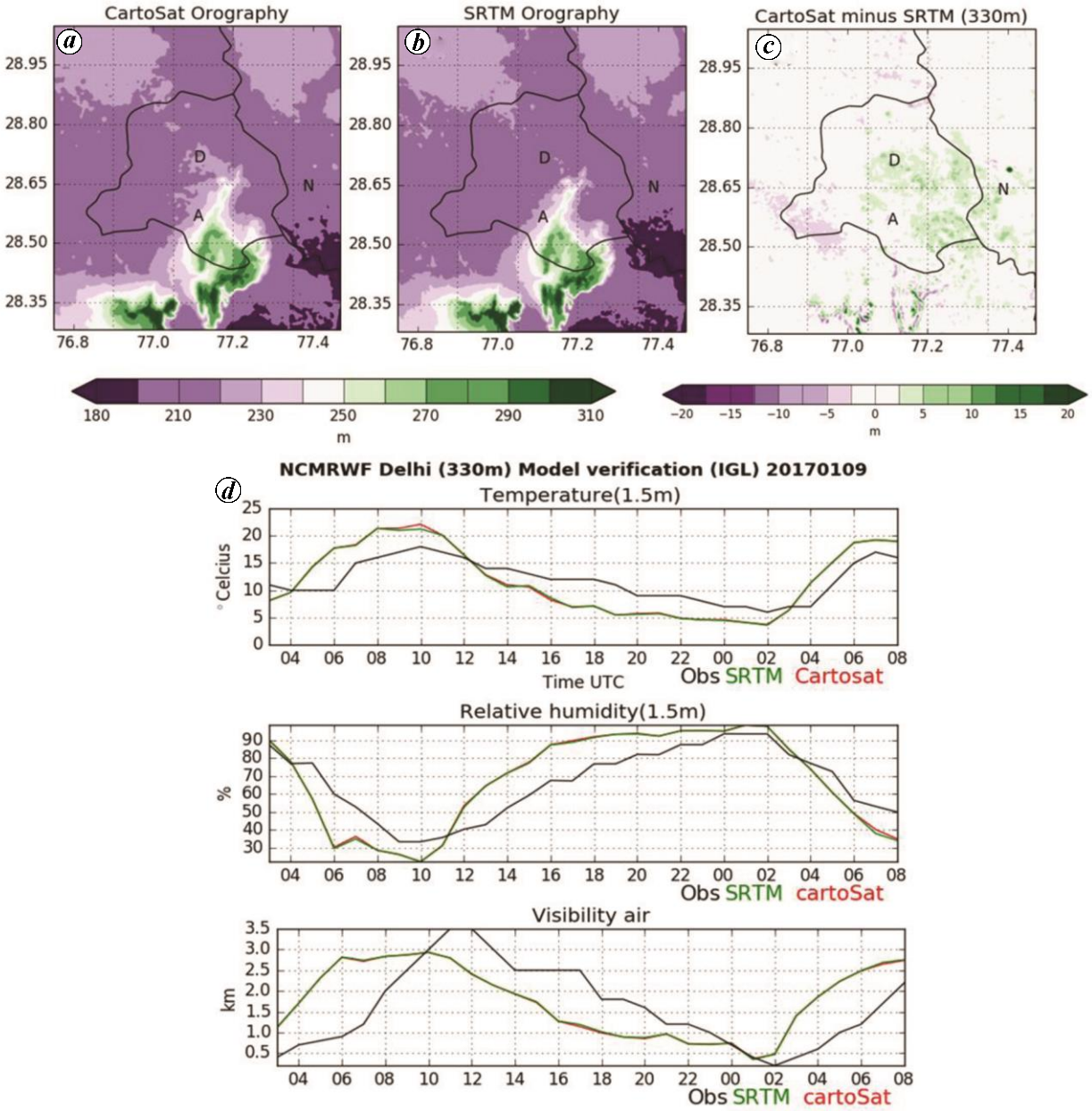

Figure 1. Orography representation of the model domain in the ancillary file derived from (***a***) Cartosat and (***b***) SRTM DEM data. (***c***) Difference between these two DEMs. The colour scale shows terrain elevation (m). (***d***) Visibility, 1.5 m temperature and relative humidity (RH) from Cartosat-run (red curve) and SRTM-run (green curve) verified against Delhi IGI airport METAR values (black curve).

with lesser (higher) relative humidity (surface temperature) bins.

Figure 4 is a 3D representation of mean orography used in Cartosat-run and SRTM-run along with the vertical velocity calculated for 950 and 850 hPa. The vertical velocity in the top panel of the figure is a manifestation of the turbulence in the topography over the DM domain. In comparison to the SRTM-run, Cartosat-run clearly indicates a higher downdraft motion for a large number of grid points (negative vertical velocity) over the total domain. Specifically, east of the Delhi ridge gives maximum downdraft area, where a larger reduction in the visibility was found in Figure 2. Vertical velocity in the lower panel of Figure 4 indicates that there are no significant changes at higher atmospheric levels due to orography modification in the model.

Weaker updraft in the nocturnal boundary layer in Cartosat-run gives a highly stable stratified and shallow boundary layer thickness (blt), compared to the SRTM-run scenario. Figure 5*a* and *b* shows the atmospheric boundary layer and wind speed forecasted during the morning hours (2 UTC). Both calm wind condition (wind speed <0.5 m/s) and cooled surface layer before sunrise result in the boundary layer with a shallow depth of

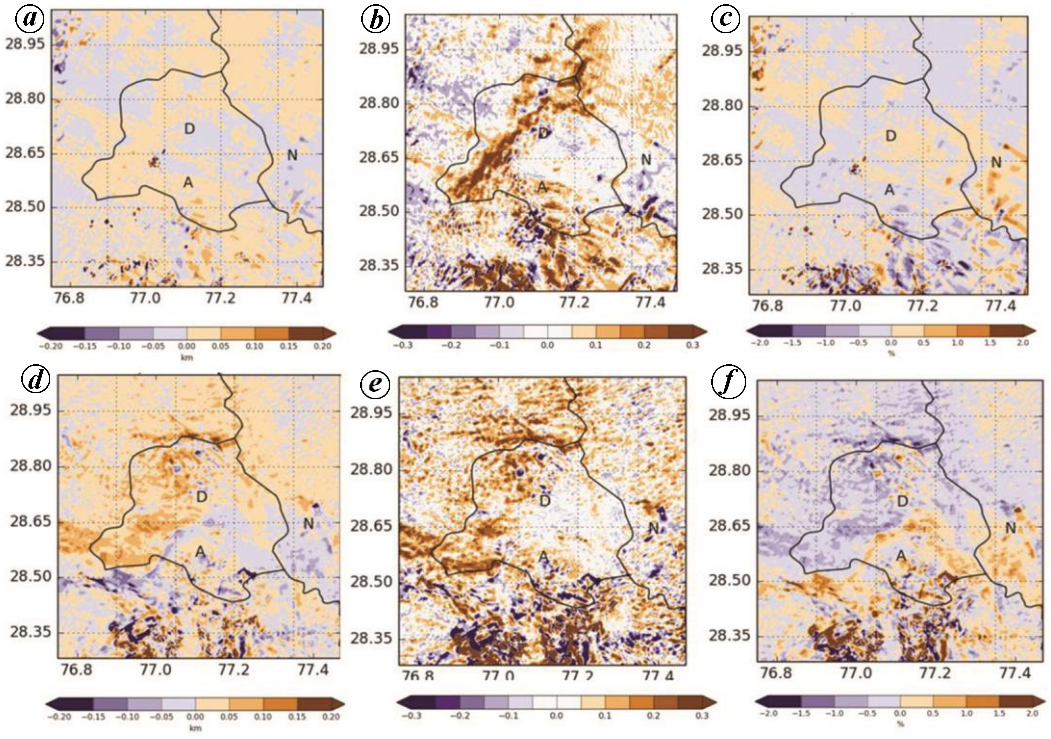

Figure 2. (***a***, ***d***) Visibility, (***b***, ***e***) temperature and (***c***, ***f***) RH difference between Cartosat-run and SRTM-run during 02UTC of 20170109 (top panel) and 20170203 (bottom panel).

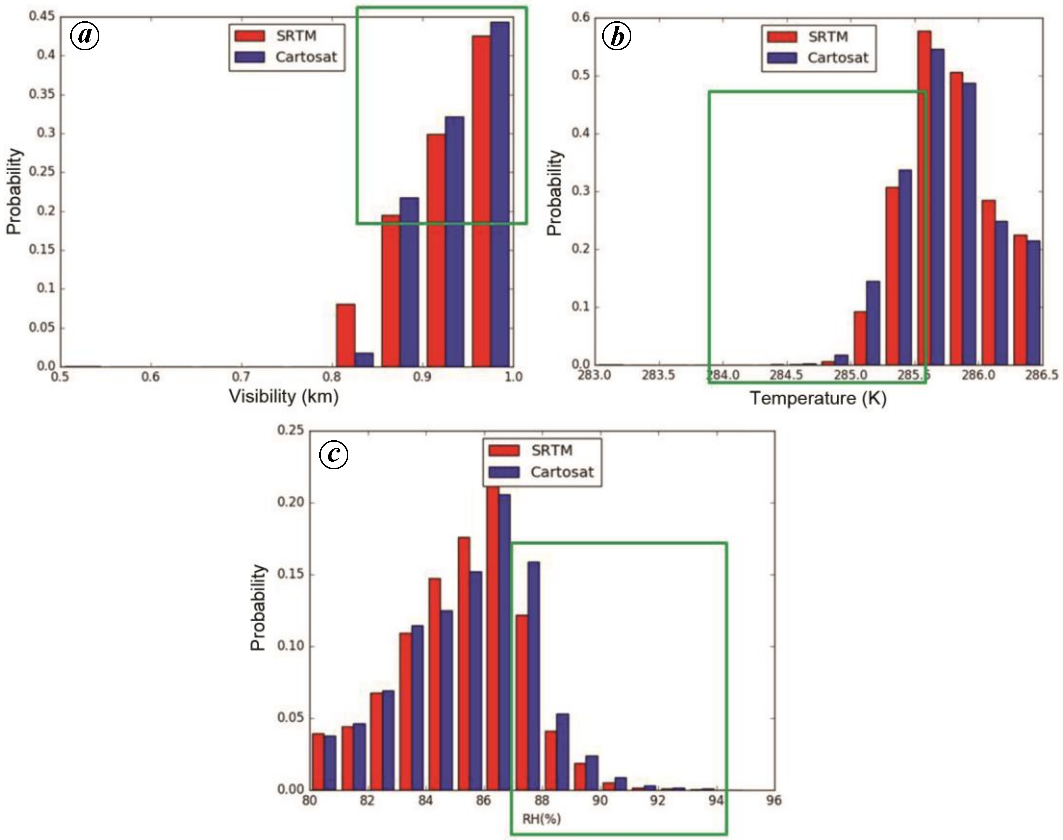

Figure 3. Histograms of (***a***) visibility, (***b***) temperature and (***c***) RH forecasted by Cartosat-run and SRTM-run during 02 UTC of 20170203. Green rectangles in each panel highlight the visibility <1.0 km, bins with surface temperature < 12.35°C and bins with RH >90%.

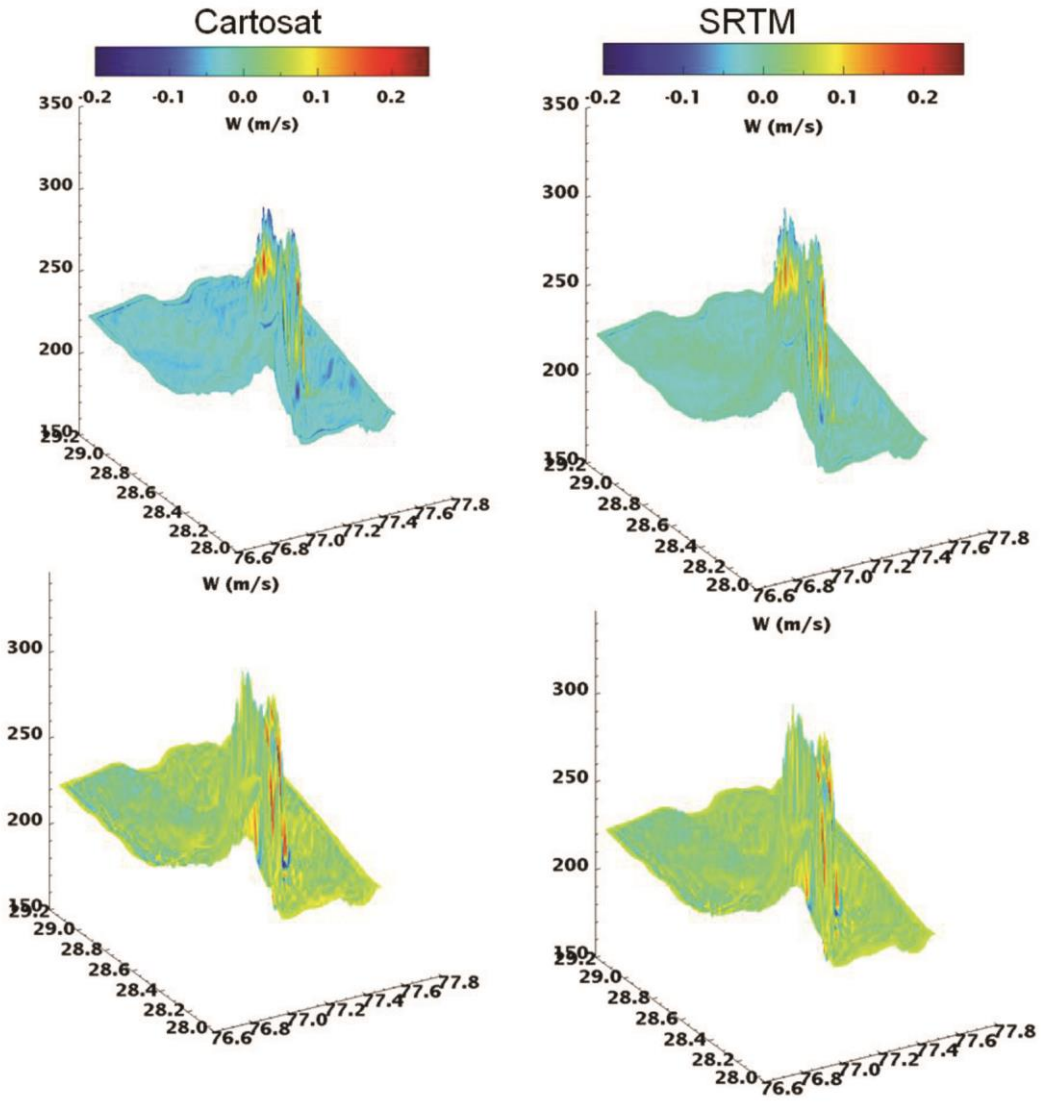

Figure 4. 3D representation of mean orography used in Cartosat-run and SRTM-run overlaid with the vertical velocity calculated for 950 hPa (top) and 850 hPa (bottom).

Table 1. Standard values for ventilation index (VI) and classification of ventilation potential based on Ferguson[8]

VI	Classification
0–235	Very poor
235–2350	Poor
2350–4700	Marginal
4700+	Good

~30 m. Aerosol is trapped in this shallow layer, which is reflected as a stable inversion layer which breaks up shortly after sunrise. The temperature profile derived from radiosonde over IGI, New Delhi (Supplementary Figure 2) shows that the inversion layer base is at around 986 hPa, which is generally in agreement with the model blt. The recent study by Nakoudi *et al.*[7] using lidar measurements for the Delhi blt (figure 3 in ref. 7) is also consistent with a shallow boundary layer in our simulations (Figure 5). Ventilation index (VI) is a good indicator of the potential of ambient atmosphere to disperse airborne pollutants. Here VI (m^2/s) from the model is calculated as

$$\mathrm{VI} = \mathrm{blt} \times V,$$

where blt (m) and V (m/s) are the boundary layer thickness and wind speed at 10 m height respectively.

Following Ferguson[8], in Table 1 the standard values of VI-based classification of atmospheric conditions are provided.

In the DM forecast during morning hours before sunrise, VI is <30 m^2/s over most of the sectors in the

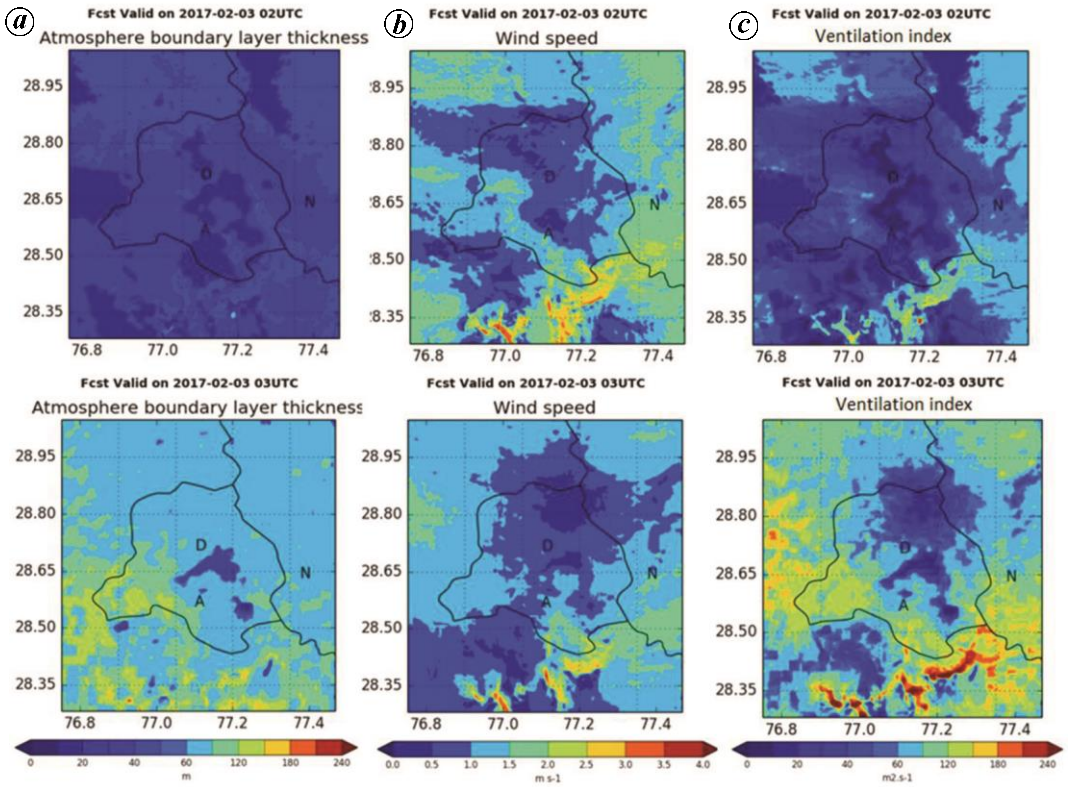

Figure 5. Atmospheric boundary layer thickness (BLT), wind speed and ventilation index (VI) for 2 UTC (top) and 3 UTC (bottom), 20170203 from Cartosat-run.

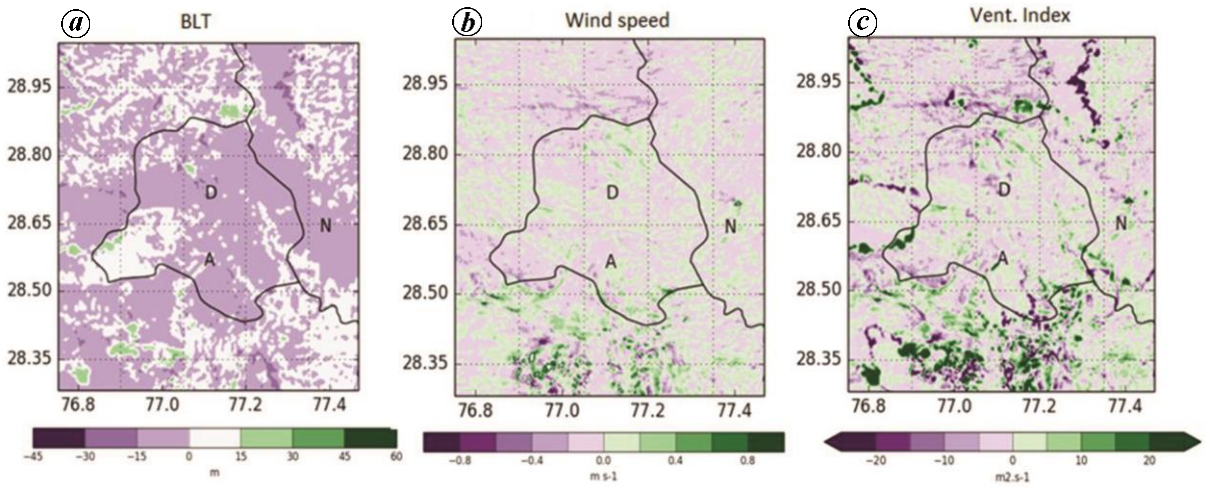

Figure 6. BLT, Wind speed and VI difference of Cartosat-run and SRTM-run during 02 UTC of 20170203.

domain, except the southern ridge of Aravalli (Figure 5 *c*), suggestive of the prevalence of 'very poor' condition that inhibit any flush-out of trapped aerosols in the shallow boundary layer. However, within almost an hour, VI is > ~200 m^2/s, except in the northern Delhi ridge sector where the UHI effect is dominant.

Figure 6 is similar to Figure 5, except that it is the difference plot (Cartosat-run minus SRTM-run) for the aforementioned variables during 02 UTC of 20170203. Figure 6 *a* clearly indicates that the thickness of blt reduce to ~20 m – through Cartosat orography implementation. This is mainly due to the reduced turbulence, and is consistent with the weak updraft velocity displayed over the area in the DM domain (Figure 4). Whereas wind speed changes are not uniform over the domain, which is highly variable and depends on both the slope and elevation changes of the two DEMs (Figure 6 *b*). With the time progression and hence the thermal mixing, the boundary layer is

>~200 m, except over the built-up regions in the domain where blt is still shallow, which is highly conditioned by UHI effect. The effect of Cartosat-1 in VI forecast is visible in Figure 6 *c*, except that the southern ridge dipole nature of index is visible in the nearby grids and majority of the grid points in the domain give reduced values in VI forecast.

In summary, the use of Cartosat-1 satellite DEM to generate orography for the DM model and its impact on the model forecast of fog/visibility-related parameters are examined. The effect of Cartosat-1 DEM through changes in the mean orography is felt at the lowest boundary layer through enhanced downdraft, and the associated push down of the boundary. In addition, the surface winds are weakened in most areas, though they are highly variable and turbulent in nature. Histogram analysis revealed enhanced fog growth through the formation of shallow boundary layer and reduced surface wind speed in the Cartosat-run. The Cartosat orography has been operationalized in the DM model since the winter season of 2018. Besides the daily operational fog/visibility forecast, the forecasting of VI from DM can serve as a potential proxy for short-range air-quality monitoring. The results presented here could be beneficial to improved air-quality risk monitoring, management and strategic planning, especially over the Delhi region.

1. Ghude, S. D., Bhat, G. S., Prabhakaran, T., Jenamani, R. K., Chate, D. M., Safai, P. D. and Rajeevan, M., Winter fog experiment over the Indo-Gangetic plains of India. *Curr. Sci.*, 2017, **112**, 767–784.
2. Gautam, R. and Singh, M. K., Urban Heat Island over Delhi punches holes in widespread fog in the Indo-Gangetic Plains. *Geophys. Res. Lett.*, 2018, **45**; https://doi.org/10.1002/2017GL076794.
3. Boutle, I. A., Price, J., Kudzotsa, I., Kokkola, H. and Romakkaniemi, S., Aerosol–fog interaction and the transition to well-mixed radiation fog, *Atmos. Chem. Phys.*, 2018, **18**, 7827–7840; https://doi.org/10.5194/acp-2017-765.
4. Jayakumar, A., Rajagopal, E. N., Boutle, I. A., George, J. P., Mohandas, S., Webster, S. and Aditi, S., An operational fog prediction system for Delhi using the 330 m Unified Model. *Atmos. Sci. Lett.*, 2018, **19**, e796; doi:10.1002/asl.796.
5. Patel, A., Katiyar, S. K., and Prasad, V., Performances evaluation of different open source DEM using differential global positioning system (DGPS). *Egypt. J. Remote Sensing Space Sci*., 2016, **19**, 7–16; doi: http://dx.doi.org/10.1016/j.ejrs.2015.12.004.
6. Sethunadh, J., Jayakumar, A., Mohandas, S. A., Rajagopal, E. N. and Nagulu, A. S., Impact of Cartosat-1 orography on weather prediction in the high resolution NCMRWF Unified Model. *J. Earth Syst. Sci.*, 2018 (accepted).
7. Nakoudi, K., Giannakaki E., Dandou, A., Tombrou, M. and Komppula, M., Planetary boundary Layer variability over New Delhi, India, during EUCAARI project, *J. Atmos. Meas. Tech.* (under review); doi: https://doi.org/10.5194/amt-2018-342.
8. Ferguson, A. S., Smoke dispersion prediction systems. In *Smoke Management Guide* (eds Hardy, C. *et al.*), National Wildlife Coordination Group, 2001, pp. 163–176.

Received 26 April 2018; revised accepted 14 December 2018

doi: 10.18520/cs/v116/i5/816-822

Hydrocarbon generation potential of source rocks in Jaisalmer Basin, Rajasthan, India

Rajesh Pandey[1,*], Dinesh Kumar[1], A. S. Maurya[1] and Pooja Pandey[2]

[1]Department of Earth Sciences, Indian institute of Technology, Roorkee 247 667, India
[2]Department of Applied Sciences, PEC University, Chandigarh 160 012, India

Geochemical and statistical analyses have been carried out for the evaluation of source rocks characteristics of Jaisalmer Basin, Rajasthan, India. The geochemical analysis includes pyrolysis data, total organic carbon, oxygen and hydrogen indices. The analysis suggests that Cretaceous source rocks are poor to fair with kerogen of types III–II and have the capability of generating gas and oil whereas the Jurassic source rocks are poor with kerogen of type III and have the capability of generating gas. The Tertiary sources of rocks however have poor potential and are immature. The Jaisalmer Basin has gas-rich petroleum system, whereas the Baisakhi–Badesir and Pariwar sources have oil generation capability. The presence of higher concentration of N_2 and CO_2 in the gas suggests the over-maturation and residual accumulation of N_2 and CO_2 in the natural gases.

Keywords: Jaisalmer Basin, kerogen, pyrolysis data, source rock.

JAISALMER Basin in the eastern part of Indus Basin has commercial production of gas in India. The available data of four tectonic units, viz. Kishangarh shelf, Jaisalmer-Mari high, Shahgarh low and Miajalar low are integrated. Maximum source rock data is available from Jaisalmer-Mari High followed by Shahgarh low and Miajlar low, while sparse data is available from Kishangarh shelf. Jaisalmer-Mari High area is operated by M/s Oil and Natural Gas Corporation (ONGC), Shahgarh low is operated by M/s Focus Energy Ltd. with ONGC as joint venture partner. Miajalar depression was operated by M/s Ente Nazionale Idrocarburi (ENI) and ONGC (now relinquished) and Kishangarh Shelf by Oil India Limited (OIL) independently.

In general, petroleum source rocks are fine-grained, organic-rich sediments that could either generate or have already generated and expelled significant amounts of petroleum[1]. The source rock potential of the basin is to be evaluated initially for assessing hydrocarbon prospectivity of the basin in terms of oil and gas. The present paper has brought out source rock geochemistry and maturity based on a compilation of studies carried out by

*For correspondence. (e-mail: rajeshbhu20@gmail.com)